NASA Technical Memorandum 84590

NASA-TM-84590 19830011807

Remote Sensing of Sediment and Chlorophyll With the Test-Bed Aircraft Multispectral Scanner

David E. Bowker, Charles A. Hardesty,
and Daniel J. Jobson

MARCH 1983

NASA

NASA Technical Memorandum 84590

Remote Sensing of Sediment and Chlorophyll With the Test-Bed Aircraft Multispectral Scanner

David E. Bowker, Charles A. Hardesty,
and Daniel J. Jobson
Langley Research Center
Hampton, Virginia

National Aeronautics
and Space Administration

**Scientific and Technical
Information Branch**

1983

SUMMARY

An instrument designed at the Langley Research Center and known as the Test-Bed Aircraft Multispectral Scanner (TBAMS) was used in a research flight over the entrance to the Chesapeake Bay on March 27, 1979. The flight followed a previous flight and took advantage of water samples already collected. Upwelled radiances from the TBAMS data were correlated with the water parameters. In particular, suspended sediment and chlorophyll *a* were used to establish initial correlations.

The instrument and scene noise levels were found to be sufficiently low to allow a 3 × 3 pixel area to average out the noise satisfactorily. In practice, however, a larger area was used because of uncertainty of station locations. Several algorithms were demonstrated for monitoring sediment and chlorophyll, with a three-band ratio being the best. The primary advantage of the three-band ratio has been found to be its insensitivity to atmospheric and Sun-angle variations.

The algorithms were used to investigate the sediment and chlorophyll profiles near the Bay entrance. There was a significant difference in the distribution of these parameters a year later, which was probably caused by low water runoff during drought conditions.

INTRODUCTION

A remote-sensing mission was conducted on March 27, 1979, near the entrance to the Chesapeake Bay. The mission was designed to satisfy experiment requirements for the Remote Airborne Fluorosensor (RAF), a laser probe designed at the Langley Research Center and used to monitor chlorophyll *a* and algae color groups. This was the first time that the laser-probe instrument had been used at an altitude of 152 m on a fixed-wing airplane, a C-54 from the Wallops Flight Center. Water samples were collected from the Bay side of the Thimble Shoals Channel to beyond the Chesapeake Light for calibration purposes. At the conclusion of the RAF experiment, the airplane conducted another pass at an altitude of 3 km over the same ocean path and data were taken with the Test-Bed Aircraft Multispectral Scanner (TBAMS), a flexible mechanical scanner with high sensitivity suitable for the remote sensing of water.

The TBAMS was designed by personnel in the Flight Electronics Division for sensor research and to support the water-quality programs at Langley. Although the system was constructed on a low budget, it offers versatility in spectral and spatial parameters and can be adapted to different detector types. The integrity of the TBAMS system had been verified on previous flights, although this occasion was the first opportunity to overfly control stations used in the calibration.

This report presents only the results of an analysis of the TBAMS data. The recorded upwelled radiances in the various spectral bands for each sampling station have been correlated with the water-parameter measurements, particularly chlorophyll *a* and suspended sediment. Emphasis has been placed on band-ratioing techniques which minimize the effects of solar elevation and off-nadir viewing. The analysis indicates the possibility of eliminating atmospheric corrections by the use of an appropriate algorithm.

TBAMS

The TBAMS is a conventional rotating mirror scanner with Cassegrainian optics and a pinhole aperture to define the image-element field of view (IFOV), which during this flight was 2 mrad. The main design features of the TBAMS system are its large size and its modular subsystems mounted on a horizontal base plate (1.22 m by 0.86 m) (which allow easy access to and replacement of the subsystems and their subcomponents). A top view of the important elements of the optical layout is shown in figure 1.

The transmission grating used for this mission had a maximum efficiency in the green region of the spectrum and was oriented with the grooved surface facing toward the collimating lens. Dispersion at the focal plane was designed to give a 20-nm bandwidth when using conventional silicon photodiodes. Spectral channels can be selected by mounting detectors and signal-processing electronics on interchangeable printed-circuit boards. The detector and preamplifier were designed to achieve the highest signal-to-noise ratio in the electronic bandwidth required for imaging.

The basic characteristics of the TBAMS are given in table I. The scanning speed is variable in fixed steps to accommodate the forward motion of the airplane in such a way that scans are contiguous. Flight data are recorded on analog tape and are later converted to a computer-compatible digital tape in the laboratory. A view of the TBAMS system with the scanner in its airplane mounting rack is given in figure 2.

It is standard practice to calibrate the TBAMS before each mission by using a National Bureau of Standards calibrated source and a magnesium carbonate diffuse reflector. The calibration procedure has been described by Jobson et al. in reference 1. Table II gives the calibration data, the center wavelength for each band and the digital counts per $\mu W/(cm^2\text{-sr-nm})$. During each scan the rotating mirror looks at an internal calibration lamp and a zero reference. This is compared with the laboratory data to verify the integrity of the system during the flight. Although the digital values can be converted to upwelled radiances by using table II, it has been found convenient to use gray-level (relative-radiance) values for data analysis.

WATER-SAMPLE DATA

Nine stations sampled during the mission were useful for correlating sea truth with the TBAMS data. The coordinates of these stations are given in table III. A sketch showing the station locations and the flight-path swath boundaries in the Chesapeake Bay entrance is presented in figure 3. The stations were sampled between 0645 and 1200, beginning with station 4 and ending with station 10. The C-54 airplane flew over this area at about 0820, thus making some of the early data over 2 hr old. In addition, maximum flood-tide current at the Chesapeake Bay Bridge occurred at 0811, which created a very dynamic environment.

The water samples were analyzed for chlorophyll *a*, salinity, and suspended sediment. These values are presented in table IV. The parameter values are plotted in figure 4 as a function of relative position along the flight path. Temperature has been included, although this parameter was not included in the data analysis. The ordinate scale is common to all values. Two items of interest are clearly seen when the data are plotted in this manner. From station 6 to station 7C there is a major increase in salinity, a slight decrease in temperature, and a significant decrease in chlorophyll. Sediment, however, remains fairly constant across this interval, but it

decreases significantly between stations 7C and 8. Thus, there appear to be at least two major water boundaries between the Chesapeake Bay Bridge and the Chesapeake Light, a chlorophyll-salinity boundary and a sediment boundary.

The water parameters were correlated with each other, and the correlation matrix is shown in table V. Some features surmised from figure 4 are also in evidence in table V: for instance, the high chlorophyll-salinity correlation and a lesser correlation between chlorophyll and sediment. (However, if station 7C were omitted, correlation would be significantly higher.) The high correlation between total sediment and its two fractions, organic and inorganic, indicates that only total sediment need be considered in the correlation analysis with upwelled radiances.

FLIGHT DATA

The C-54 airplane flew from west to east along the flight path shown in figure 3 at a nominal altitude of 3000 m and a velocity of 246 km/hr. An image of the area from stations 4 to 7C, generated with band-4 radiance values, is shown in figure 5. The flood-tide current patterns around the channel entrance are well defined, and a surface line boundary between the two water masses near station 7C is also visible. The herringbone striping (sinusoidal pattern) seen running from left to right was due to servo-noise pickup and was filtered from the data before analysis; averaging a number of pixels also helped to minimize its effect.

The pixel number for each station was located in the band-4 gray-level printout with the aid of airplane photography and marine charts by using boat and buoy positions as reference points. Before radiance values were extracted from the data, a study was made of the standard deviation as the station sample size grew by $(n)^2$ pixels, where n is the number of pixels along and across the scan lines. A plot of the standard deviation σ as a function of n for two representative bands (4 and 6) is shown in figures 6 and 7, respectively, for stations 8, 9, and 10. These three stations are in deep water and are relatively free of scene variations. It is apparent that a 3 × 3 pixel area is sufficient to minimize the noise produced by the scanner electronics and the ocean surface. However, the uncertainty in locating each station, the time between the water-sample collection and the overflight, and the dynamics of the water during maximum flood-tide current suggest that a larger sample is desirable. For this analysis, then, a 10 × 10 pixel area was used to obtain the upwelled radiances at each station.

When radiance data are obtained over a uniform target, there is an increase in radiance away from nadir. This is generally due to the increase in atmospheric pathlength and Sun-angle variations. If correlations are to be attempted between water parameters and single radiance values, there must be a correction applied to remove the off-nadir variation. This correction is obtained by averaging many scan lines along the flight track, usually from areas that contain a minimum of scene detail. The corrected radiance values for each station are given in table VI. These are gray-level values used in the data analysis; they can be converted to $\mu W/(cm^2\text{-sr-nm})$ by using the calibration data in table II.

DATA ANALYSIS

The upwelled radiances from the nine stations have been correlated with the sediment and chlorophyll values. These data are presented in table VII for three-band ratios, two-band ratios, and single bands. Band 4 (B4), the brightest band, has

the best correlation with sediment, whereas band 5 (B5) has the best correlation with chlorophyll. The low correlations with band 2 are due to the low sensitivity of the silicon detectors and the increased atmospheric scattering in the blue region of the spectrum.

Since single-band correlations are dependent on illumination levels, it is necessary to correct for Sun elevation and varying sky conditions when the flight extends over a period of time or long distances. By ratioing bands (B), the Sun elevation and atmospheric variations can be minimized. The ratios presented here are of the form B_i/B_{i+1} for the two-band case and $B_i^2/(B_{i-1})(B_{i+1})$ for the three-band case. The ratios eliminate the need for Sun-elevation corrections and also minimize the atmospheric influence when the scattering and absorption variations for the bands are correlated.

The best two-band ratio for remote sensing is B7/B8 for sediment and B5/B6 for chlorophyll. When these bands are converted to the three-band algorithm by multiplying by B_i/B_{i-1}, the correlation improves slightly as shown in table VII. A more complete description of the application of this particular algorithm to remote sensing of water has been given by Grew in reference 2.

The influence of sediment and chlorophyll on the upwelled radiances can be seen in the normalized response of TBAMS over two stations with large differences in the parameters. Figure 8 shows the normalized radiance data for stations 5 and 10. The sediment at these stations differs by 8.5 mg/L, and the chlorophyll differs by 17.6 μg/L. The large variation in band 8 relative to band 7 is due primarily to sediment, whereas the variation in band 5 relative to band 6 is influenced more by chlorophyll. The three-band algorithm is equivalent to the angular variation of the normalized response about the central band. For example, in figure 8, sediment correlates with the angle ϕ where

$$\phi = 180 - \tan^{-1}[(B6 - B7)/0.1] - \tan^{-1}[(B8 - B7)/0.1]$$

Of course, the angle ϕ is sensitive to the scale used in the normalized plot.

Figure 9 is a plot of the sediment data as a function of the radiance ratio B7/B8. The equation for the regression line is also given. A similar plot for the ratio $(B7)^2/(B6 \times B8)$ is shown in figure 10. The scatter among the high-sediment values in figures 9 and 10 is influenced by the time displacement between the sampling and overflight and the dynamics of the marine environment. This condition is typical for most estuarine remote-sensing missions when sampling is done over large areas by using a ship.

A plot of $(B5)^2/(B4 \times B6)$ as a function of the chlorophyll values is given in figure 11. These data show some clustering at the extreme ends of the chlorophyll range. It has been shown previously in reference 3 that the low values of chlorophyll (<6 μg/L) are better represented by the algorithm $(B4)^2/(B3 \times B5)$. These data are plotted in figure 12 where it appears that the algorithm is limited to values below about 6 μg/L. When the log of the chlorophyll values is used instead of chlorophyll, the coefficient of correlation increases to 0.995.

The sediment algorithm, $(B7)^2/(B6 \times B8)$, and chlorophyll algorithms, $(B5)^2/(B4 \times B6)$ for values greater than 6 μg/L and $(B4)^2/(B3 \times B5)$ for values less than 6 μg/L, have been applied to the TBAMS data to generate a profile of the param-

eters near the entrance to the Chesapeake Bay. Figures 13 and 14 were obtained by using a 25 × 25 pixel element at nadir between the Chesapeake Bay Bridge and the Chesapeake Light. There is a sharp drop in chlorophyll near the 15-km mark, whereas sediment declines gradually from 22 km seaward. This is in agreement with the sea truth: station 7C indicates the presence of a transition region between the Chesapeake Bay plume and clear ocean water, where chlorophyll *a* is low but sediment is still high. Beyond the Light both parameters assume a more constant value. These data contrast markedly with data taken a year later (ref. 3) when both parameters were very low because of a prolonged drought in the area. The maximum sediment and chlorophyll values along the same track were about 3 mg/L and 6 μg/L, respectively.

CONCLUDING REMARKS

The Test-Bed Aircraft Multispectral Scanner (TBAMS) was designed to be a flexible research instrument for investigating spectral reflectances. During this research mission it was found to be satisfactory for remote sensing of the low upwelled regions of the marine environment. Therefore, one of the objectives, to demonstrate the application of a cost-effective scanner, was satisfied.

The two algorithms $(B4)^2/(B3 \times B5)$ and $(B5)^2/(B4 \times B6)$, where B represents band, were found to be very effective for remote sensing of low and high values of chlorophyll, respectively. The low-chlorophyll algorithm is very sensitive to the blue-green absorption region, whereas the high-chlorophyll algorithm is responsive to the green-reflectance peak. The algorithm $(B7)^2/(B6 \times B8)$ was the best for monitoring sediment. This seems somewhat unusual since band 7 (centered at 680 nm) is located in the chlorophyll absorption area and band 8 (centered at 712 nm) is located in the near-infrared reflectance region for vegetation. These algorithms have been successful on other missions, however, when the correlation between chlorophyll and sediment was less.

The three-band algorithm offers the potential advantage of being less sensitive to atmospheric and Sun-angle variations. This could not be confirmed by the data presented here because of the small number of calibration samples and the fairly uniform flight conditions. The insensitivity of the algorithms to varying altitudes, flight directions, and off-nadir scan angles was confirmed in a later mission described by Bowker et al. in NASA CP-2188.

Langley Research Center
National Aeronautics and Space Administration
Hampton, VA 23665
January 21, 1983

REFERENCES

1. Jobson, Daniel J.; Hardesty, Charles A.; Katzberg, Stephen J.; and Burcher, Ernest E.: Radiometric Performance of the Test-Bed Aircraft Multispectral Scanner (TBAMS) System. Opt. Eng., vol. 20, no. 5, Sept./Oct. 1981, pp. 772-776.

2. Grew, Gary W.: Characteristic Vector Analysis as a Technique for Signature Extraction of Remote Ocean Color Data. Remote Sensing of Earth Resources - Volume VI, F. Shahrokhi, ed., Univ. Tennessee, Space Inst., c.1977, pp. 109-144.

3. Bowker, David E.; Hardesty, Charles A.; Jobson, Daniel J.; and Bahn, Gilbert S.: Analysis of Testbed Airborne Multispectral Scanner Data From Superflux II. Chesapeake Bay Plume Study - Superflux 1980, Janet W. Campbell and James P. Thomas, eds., NASA CP-2188, NOAA/NEMP III 81 ABCDFG 0042, 1981, pp. 323-337.

TABLE I.- BASIC CHARACTERISTICS OF THE TBAMS

IFOV, deg	0.113
Swath angle, deg	61.8
Number of pixels per line	703
Pixel-sampling overlap	1.28
Number of visible bands	8
Bandwidth, nm	20

TABLE II.- CENTER WAVELENGTH AND RADIANCE CALIBRATION FOR EACH VISIBLE NEAR-INFRARED BAND

Band	Center wavelength, nm	Calibration, counts per $\mu W/(cm^2\text{-}sr\text{-}nm)$
2	470	11.9
3	512	31.1
4	558	54.5
5	600	55.9
6	640	64.7
7	680	56.5
8	712	65.5

TABLE III.- COORDINATES OF STATIONS USED FOR WATER-SAMPLE ANALYSIS

Station	Latitude	Longitude
3A	36°58.7' N	76°08.5' W
4	36°58.35' N	76°08.6' W
1F	36°58.5' N	76°07.0' W
5	36°57.15' N	76°01.85' W
6	36°56.2' N	75°57.5' W
7C	36°55.55' N	75°54.65' W
8	36°54.5' N	75°43.0' W
9	36°52.75' N	75°30.5' W
10	36°50.66' N	75°12.0' W

TABLE IV.- WATER-PARAMETER VALUES MEASURED AT EACH STATION

Water parameter	Water-parameter values at station -								
	3A	4	1F	5	6	7C	8	9	10
Chlorophyll a, μg/L	16.00	15.25	15.00	19.00	13.00	2.70	1.90	1.80	1.40
Salinity, ppt	16.00	18.00	16.50	17.00	19.00	27.00	27.00	28.00	31.00
Organic sediment, mg/L	5.60	4.70	2.90	4.10	4.20	5.00	1.90	2.70	2.40
Inorganic sediment, mg/L	7.10	7.10	4.50	7.90	5.20	5.80	0.40	1.20	1.10
Total sediment, mg/L	12.70	11.90	7.40	12.00	9.40	10.80	2.30	3.80	3.50

TABLE V.- CORRELATION MATRIX FOR THE WATER PARAMETERS

	1	2	3	4	5
1. Chlorophyll a	1.000				
2. Salinity	.971	1.000			
3. Organic sediment	.556	.567	1.000		
4. Inorganic sediment	.832	.798	.876	1.000	
5. Total sediment	.768	.747	.939	.989	1.000

TABLE VI.- CORRECTED RADIANCE GRAY LEVELS FOR EACH BAND AT EACH STATION

Station	Gray levels for band -						
	2	3	4	5	6	7	8
3A	22.74	37.49	103.87	71.62	72.20	32.33	43.08
4	22.67	38.45	106.37	73.74	74.69	34.05	43.20
1F	21.25	34.99	92.23	65.10	66.84	29.39	39.25
5	22.52	36.95	100.62	72.60	73.58	32.39	40.53
6	23.30	36.95	100.71	70.06	71.80	32.35	43.99
7C	23.26	37.50	100.28	66.25	68.79	30.79	41.32
8	21.43	33.74	84.62	57.13	60.89	26.17	39.55
9	23.01	34.16	85.87	58.06	62.39	26.82	39.89
10	23.56	35.70	84.25	57.82	60.97	26.79	39.72

TABLE VII.- CORRELATIONS OF SEDIMENT AND CHLOROPHYLL a WITH VARIOUS BAND COMBINATIONS

Water parameter	Correlations of three-band ratios -				
	$(B3)^2/(B2 \times B4)$	$(B4)^2/(B3 \times B5)$	$(B5)^2/(B4 \times B6)$	$(B6)^2/(B5 \times B7)$	$(B7)^2/(B6 \times B8)$
Sediment	-0.498	0.781	0.697	-0.912	0.944
Chlorophyll a	-.315	.418	.965	-.780	.829

Water parameter	Correlations of two-band ratios -					
	B2/B3	B3/B4	B4/B5	B5/B6	B6/B7	B7/B8
Sediment	-0.793	-0.900	-0.356	0.916	-0.806	0.923
Chlorophyll a	-.781	-.788	-.822	.910	-.545	.859

Water parameter	Correlations of single bands -						
	B2	B3	B4	B5	B6	B7	B8
Sediment	0.182	0.898	0.972	0.961	0.959	0.954	0.693
Chlorophyll a	.230	.558	.737	.872	.845	.807	.469

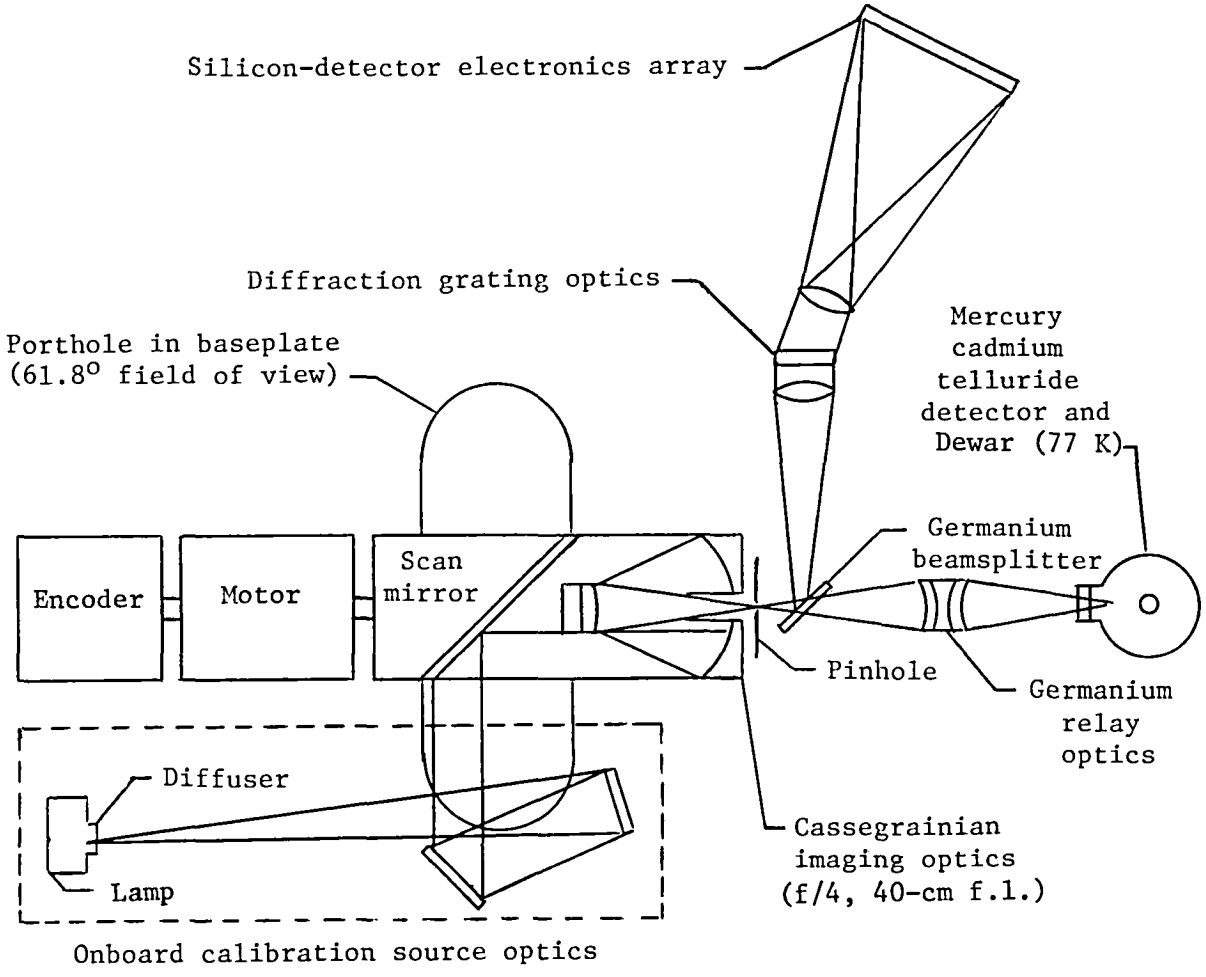

Figure 1.- Top view of layout showing important elements of TBAMS.

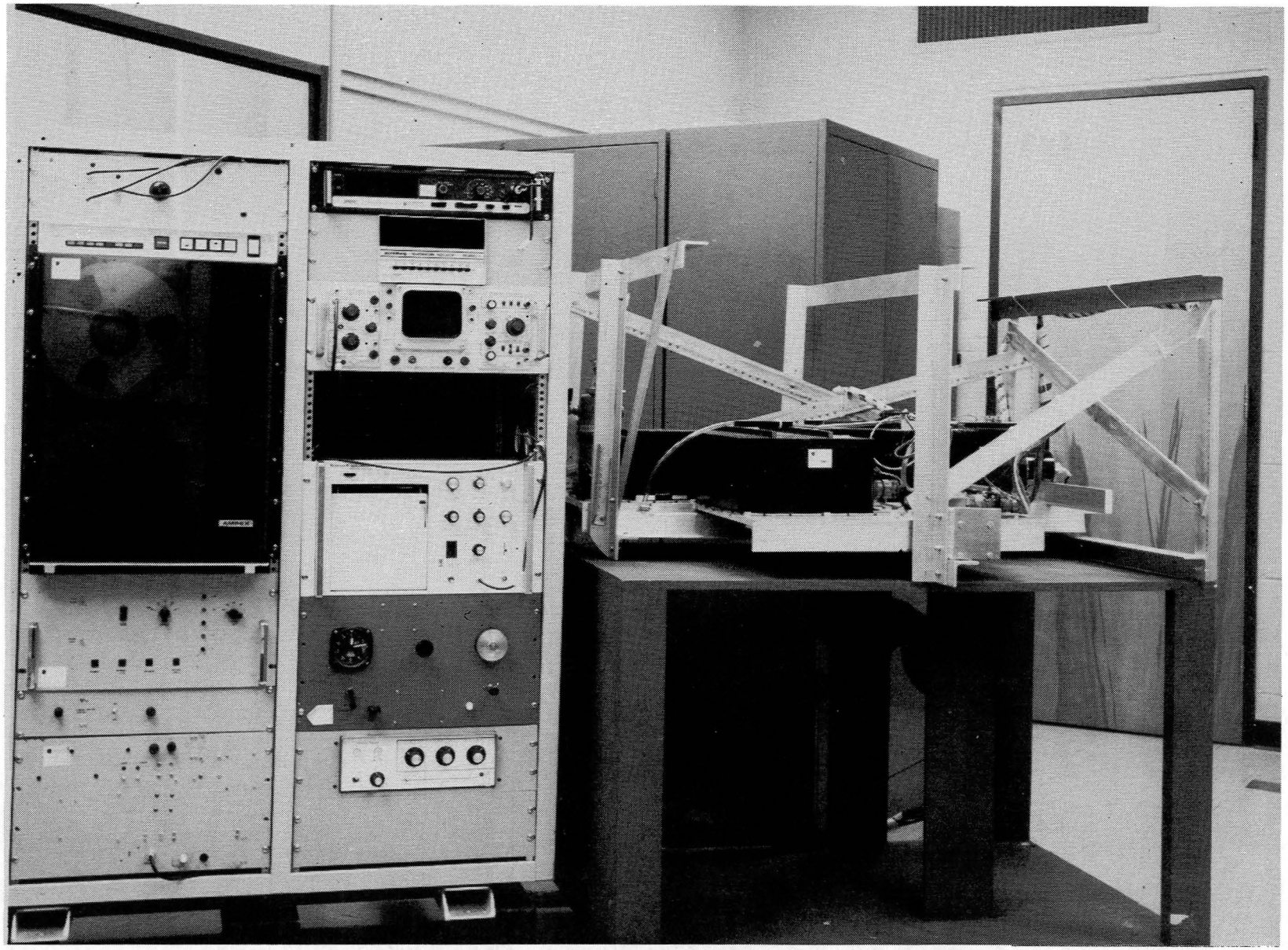

L-80-5549

Figure 2.- View of TBAMS system with scanner in its airplane mounting rack.

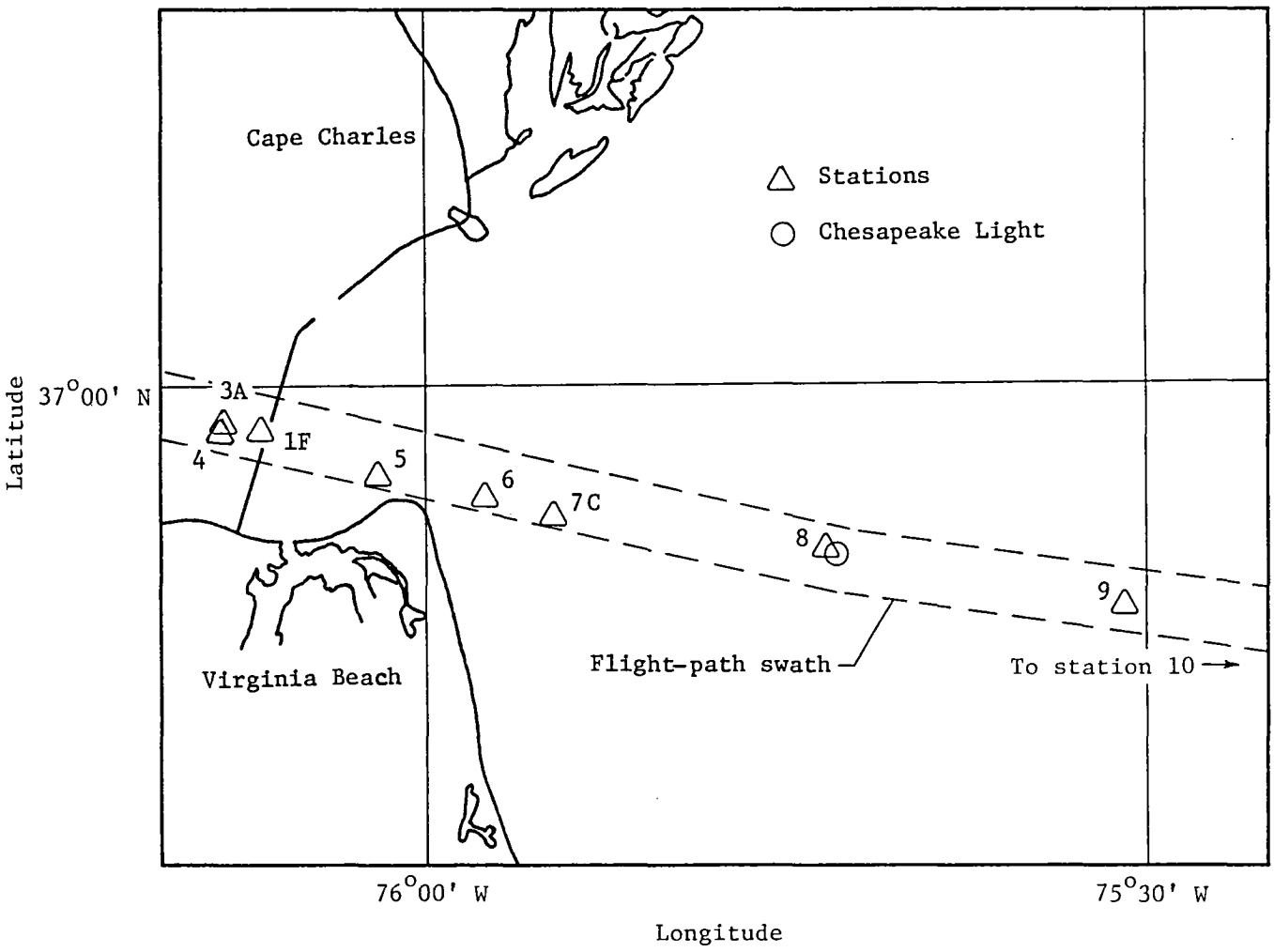

Figure 3.- Sketch showing station locations and flight-path swath boundaries in the Chesapeake Bay entrance.

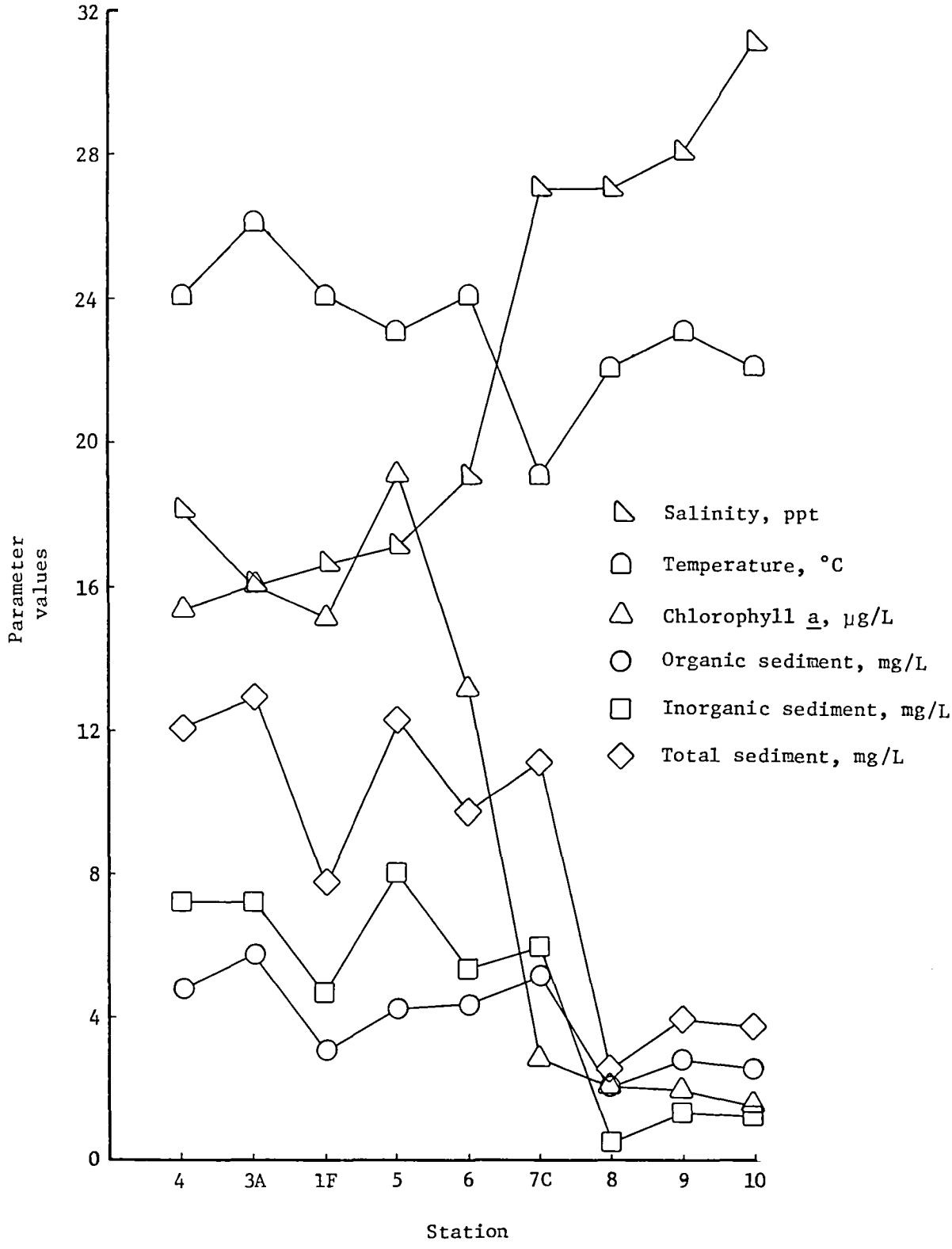

Figure 4.- Plot of station parameters as a function of relative station position along flight path.

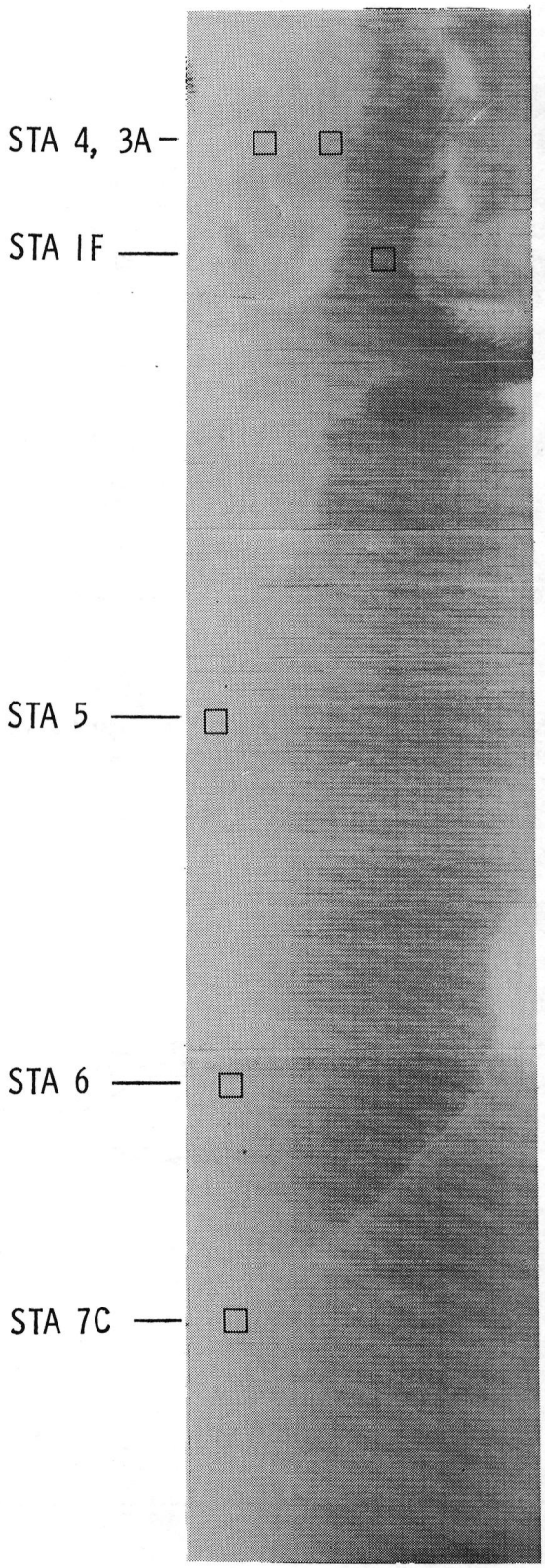

L-83-09

Figure 5.- Image of flight path from station 4 to station 7C generated with band-4 radiance values of TBAMS.

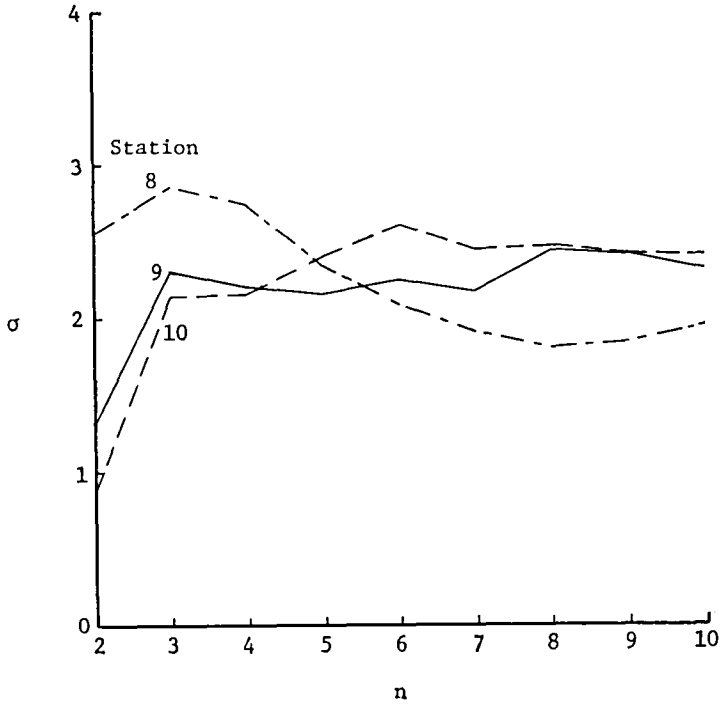

Figure 6.- Standard deviation of band-4 radiance values as a function of $(n)^2$ pixel area for stations 8, 9, and 10.

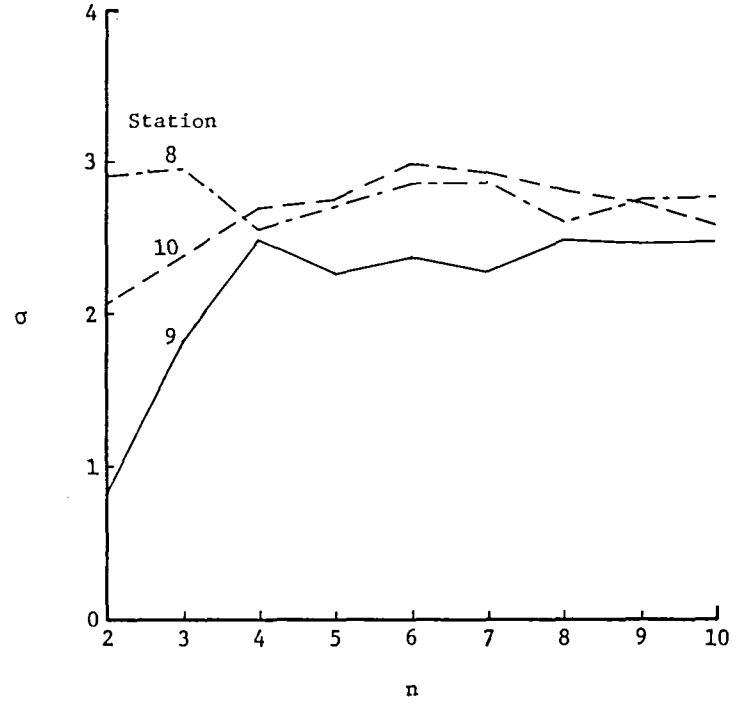

Figure 7.- Standard deviation of band-6 radiance values as a function of $(n)^2$ pixel area for stations 8, 9, and 10.

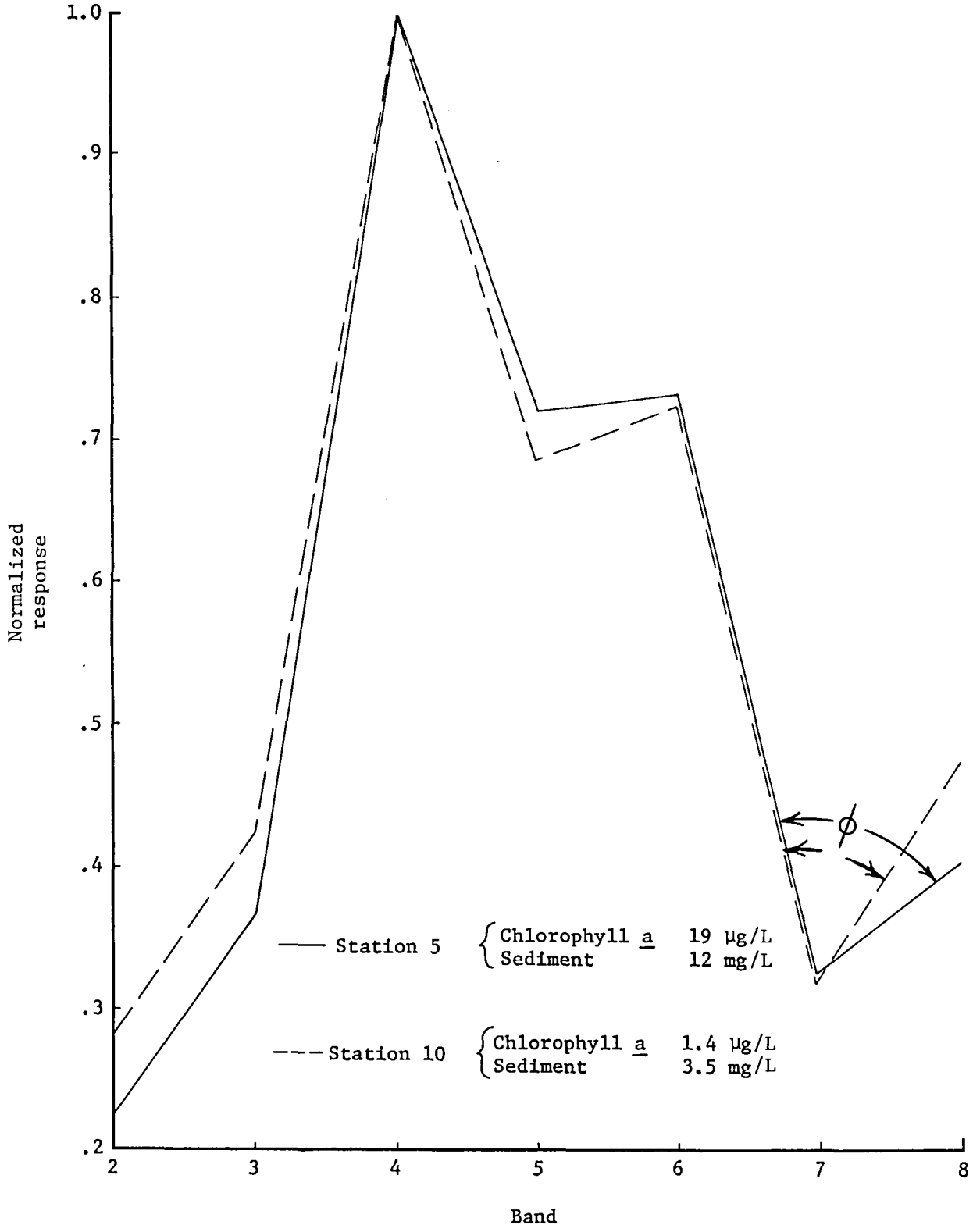

Figure 8.- Normalized response of TBAMS at stations 5 and 10.

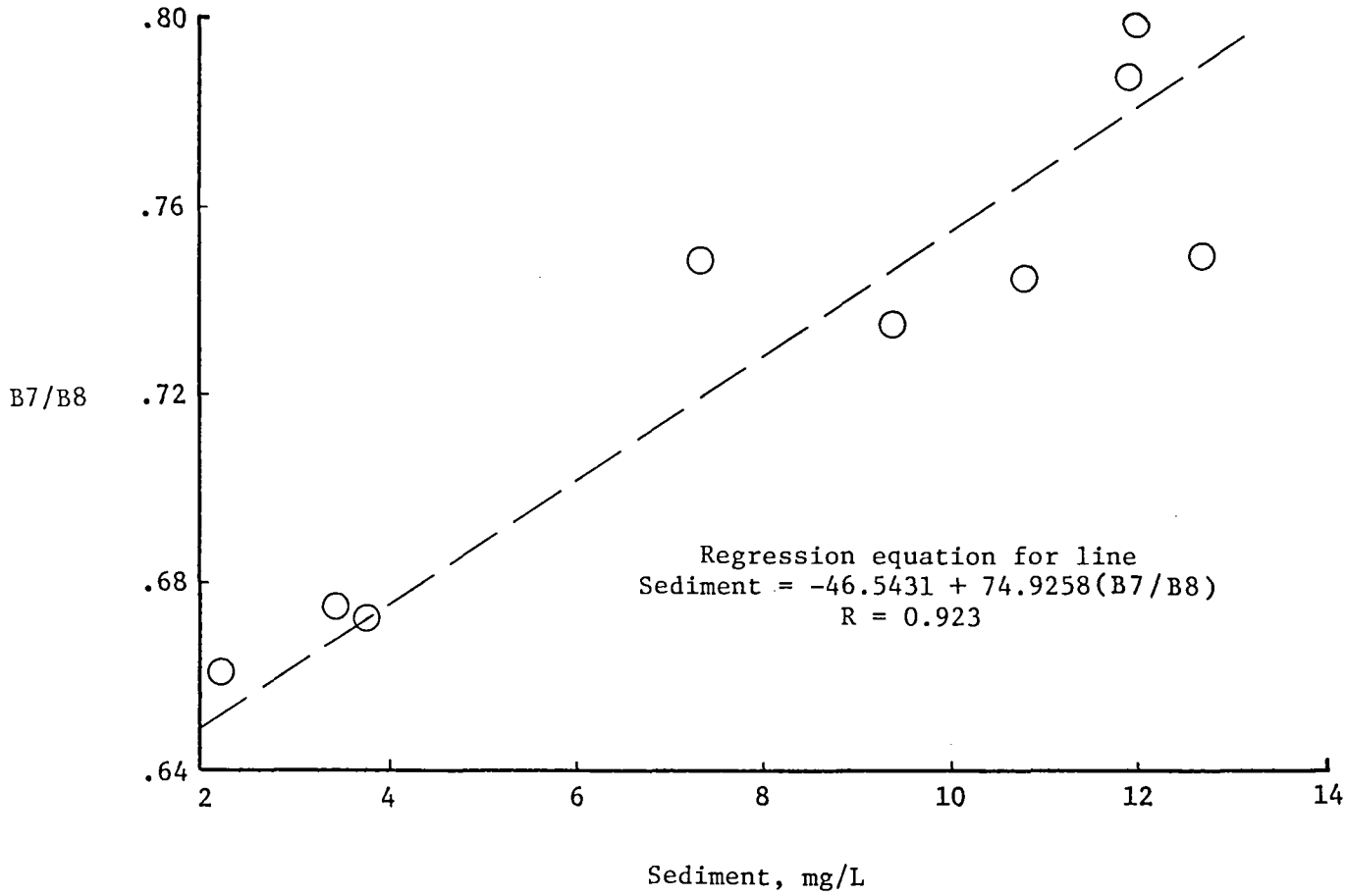

Figure 9.- Plot of B7/B8 as a function of sediment showing regression line and giving regression equation and coefficient of correlation R.

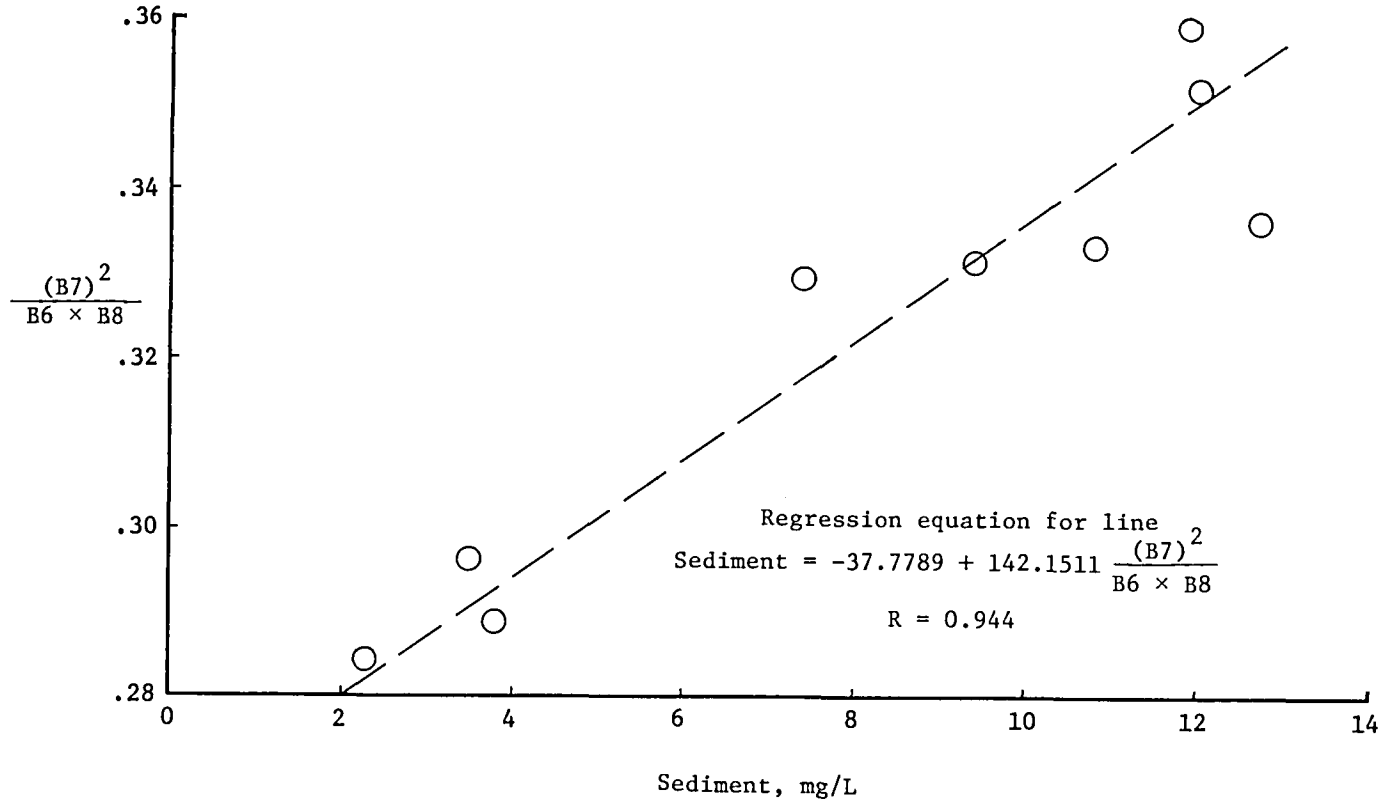

Figure 10.- Plot of $(B7)^2/(B6 \times B8)$ as a function of sediment showing regression line and giving regression equation and coefficient of correlation R.

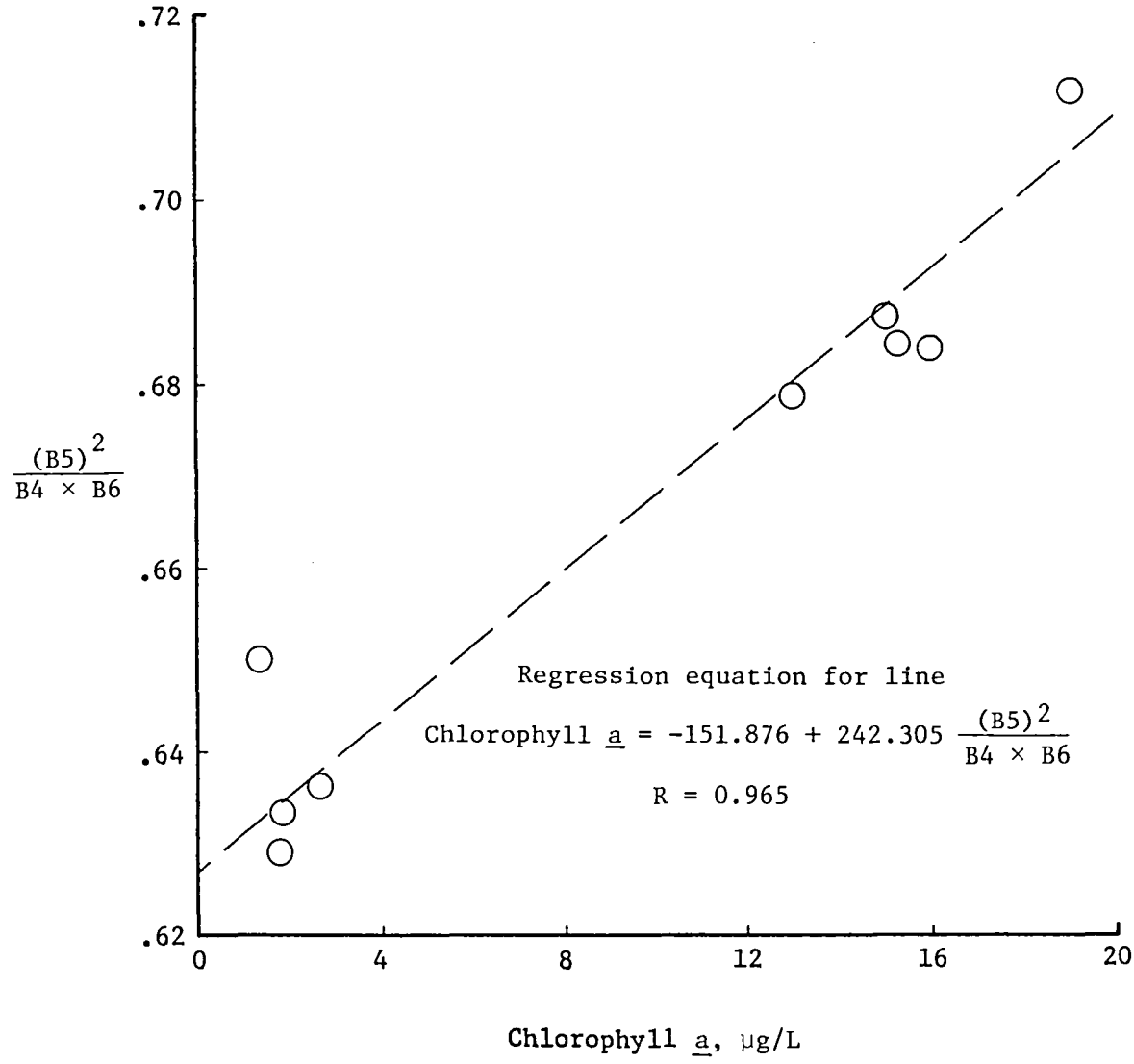

Figure 11.- Plot of $(B5)^2/(B4 \times B6)$ as a function of chlorophyll a showing regression line and giving regression equation and coefficient of correlation R.

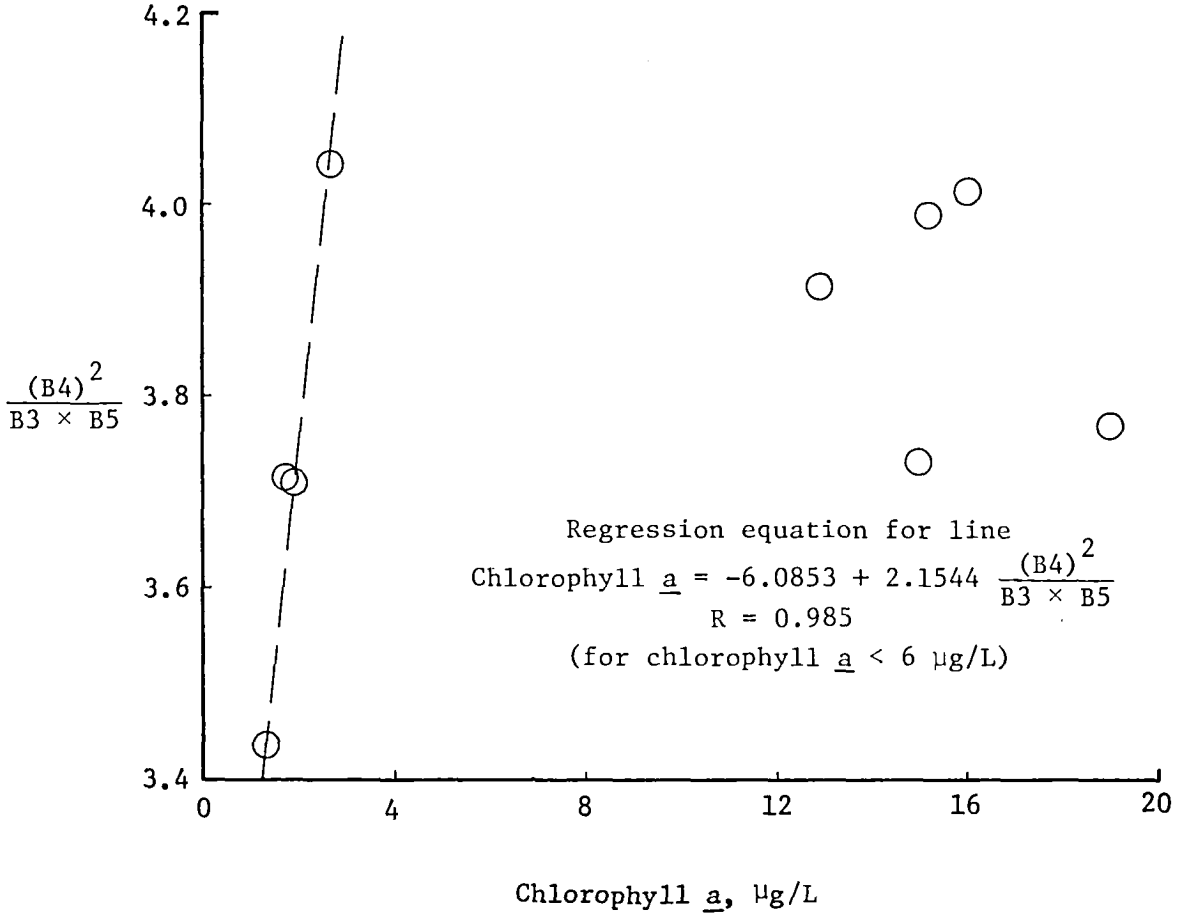

Figure 12.- Plot of $(B4)^2/(B3 \times B5)$ as a function of chlorophyll a showing regression line and giving regression equation and coefficient of correlation R.

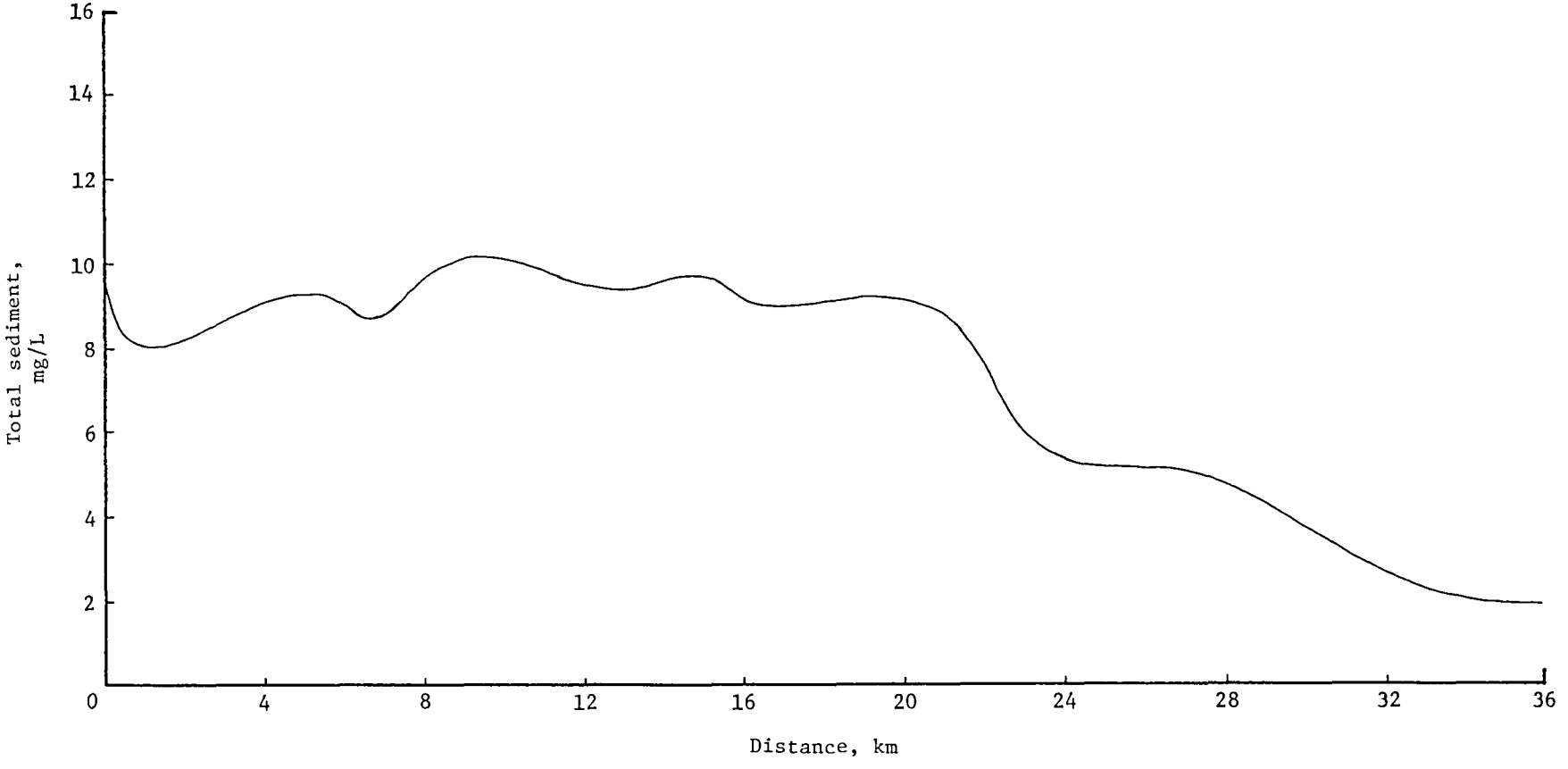

Figure 13.- Plot of total sediment derived from TBAMS nadir radiance as a function of distance from the Chesapeake Bay Bridge to the Chesapeake Light.

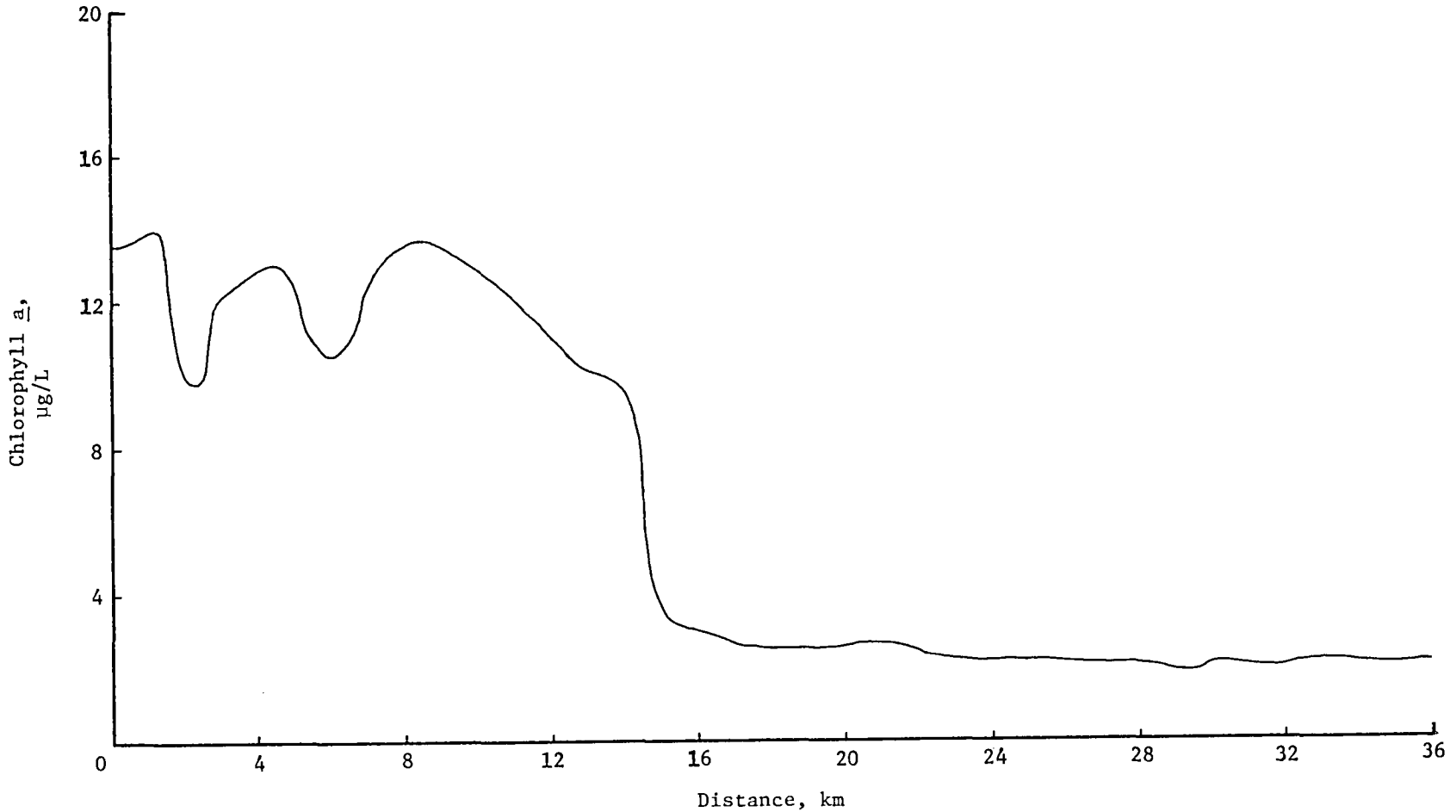

Figure 14.- Plot of chlorophyll a derived from TBAMS nadir radiance as a function of distance from the Chesapeake Bay Bridge to the Chesapeake Light.

1. Report No.	2. Government Accession No.	3. Recipient's Catalog No.
NASA TM-84590		

4. Title and Subtitle	5. Report Date
REMOTE SENSING OF SEDIMENT AND CHLOROPHYLL WITH THE TEST-BED AIRCRAFT MULTISPECTRAL SCANNER	March 1983
	6. Performing Organization Code: 506-61-03-01

7. Author(s)	8. Performing Organization Report No.
David E. Bowker, Charles A. Hardesty, and Daniel J. Jobson	L-15572
	10. Work Unit No.

9. Performing Organization Name and Address	11. Contract or Grant No.
NASA Langley Research Center Hampton, VA 23665	
	13. Type of Report and Period Covered: Technical Memorandum

12. Sponsoring Agency Name and Address	14. Sponsoring Agency Code
National Aeronautics and Space Administration Washington, DC 20546	

15. Supplementary Notes

16. Abstract

An instrument designed at the Langley Research Center and known as the Test-Bed Aircraft Multispectral Scanner (TBAMS) was used in a research flight over the entrance to the Chesapeake Bay on March 27, 1979. Upwelled radiances from the TBAMS data were correlated with the water parameters, particularly sediment and chlorophyll a. Several algorithms were demonstrated for monitoring sediment and chlorophyll, with a three-band ratio being the best. The primary advantage of the three-band ratio has been found to be its apparent insensitivity to atmospheric and Sun-angle variations.

17. Key Words (Suggested by Author(s))	18. Distribution Statement
Instrumentation Remote sensing Statistical analysis Correlations Marine upwelled radiance	Unclassified - Unlimited Subject Category 35

19. Security Classif. (of this report)	20. Security Classif. (of this page)	21. No. of Pages	22. Price
Unclassified	Unclassified	24	A02

For sale by the National Technical Information Service, Springfield, Virginia 22161 NASA-Langley, 1983

National Aeronautics and
Space Administration

Washington, D.C.
20546

Official Business
Penalty for Private Use, $300

THIRD-CLASS BULK RATE

Postage and Fees Paid
National Aeronautics and
Space Administration
NASA-451

POSTMASTER: If Undeliverable (Section 158 Postal Manual) Do Not Return